CELL CYCLE
2021, VOL. 20, NO. 20, 2137–2148
https://doi.org/10.1080/15384101.2021.1971351

Taylor & Francis
Taylor & Francis Group

RESEARCH PAPER

Long non-coding RNA NORAD induces phenotypic regulation of vascular smooth muscle cells through regulating microRNA-136-5p-targeted KDM1A

Chao Lv[#], Jun Wang[#], Shuhui Dai, Yanwei Chen, Xiaofan Jiang, and Xia Li

Department of Neurosurgery, The First Affiliated Hospital of Airforce Medical University, Xi'an Shaanxi, China

ABSTRACT

Objective: Effect of long non-coding RNAs (lncRNAs) on intracranial aneurysm (IA) development has been identified, while the role of noncoding RNA activated by DNA damage (NORAD) in IA remains unexplored. We aimed to verify the impact of NORAD on IA through sponging microRNA-136-5p (miR-136-5p).

Methods: Ruptured and unruptured IAs were harvested from IA patients, and expression of NORAD, miR-136-5p, and KDM1A was determined. The vascular smooth muscle cells (VSMCs) were cultured and, respectively, transfected with altered NORAD, miR-136-5p, or lysine-specific demethylase 1 (KDM1A) to observe their effect on biological functions, as well as on contraction and synthesis-specific indices of VSMCs. Interactions between NORAD and miR-136-5p, and between miR-136-5p and KDM1A were confirmed.

Results: NORAD and KDM1A were upregulated while miR-136-5p was downregulated in IA, especially in ruptured IA. NORAD overexpression or miR-136-5p inhibition accelerated proliferation and migration, and decelerated phenotypic switching and apoptosis of VSMCs. The effects of overexpressed NORAD on VSMCs were reserved by miR-136-5p upregulation or KDM1A knockdown. NORAD functioned as a competing endogenous RNA of miR-136-5p and miR-136-5p targeted KDM1A.

Conclusion: NORAD suppressed miR-136-5p, thus upregulating KDM1A to participate in IA formation and rupture by inducing phenotypic regulation of VSMCs.

ARTICLE HISTORY
Received 23 September 2020
Revised 25 April 2021
Accepted 31 May 2021

KEYWORDS
Intracranial aneurysm; Noncoding RNA activated by DNA damage; microRna-136-5p; lysine-specific demethylase 1a; formation and rupture; vascular smooth muscle cell

Introduction

Referring to an abnormal focal dilatation of the intracranial artery [1], intracranial aneurysm (IA) is a severe issue presenting with rupture and compressive impacts [2]. IA is featured by local structural degradation of the arterial wall, with diminishment of the internal elastic lamina and disruption of the media [3]. IA affects around 1–5% of the general population and the ruptured IA is a leading cause of nontraumatic subarachnoid hemorrhage, which can result in serious disability or even death [4]. Genetic and environmental risk factors are reported to be associated with IA formation, while the molecular pathology of IA remains largely unknown [5]. Technology development has facilitated the therapeutic strategies of vascular disorders affecting the central nervous system such as IA [6]. Nevertheless, these treatments, including preventive endovascular or microsurgical occlusion, carry complication risks [7], and a recurrence may appear in the future [8]. Therefore, novel targets are urgently demanded for IA treatment.

Long non-coding RNAs (lncRNAs) are non-coding RNAs lacking protein-coding capacity [9]. LncRNAs play essential roles in IA, such as TCONS_00000200 [10] and GASL1 [11]. Noncoding RNA activated by DNA damage (NORAD), one of the lncRNAs, has been reported to participate in tumor development. For instance, NORAD played a pivotal function on colorectal cancer (CRC) progression [12], and it has also been demonstrated that NORAD promoted breast cancer development [13]. Nevertheless, the role of NORAD in IA has been scarcely explored. MicroRNAs (miRNAs) are non-coding RNAs

CONTACT Xia Li Lixia958@tom.com Department of Neurosurgery, The First Affiliated Hospital of Airforce Medical University, Xi'an Shaanxi, China

[#]These authors are co-first authors.

that suppress the translation and stability of mRNAs and control genes associated with cell processes. MiRNAs can modulate protein expression by binding 3′-untranslation region (3′-UTR) in the target mRNA [14]. Several particular miRNAs were identified in IA progression, such as miR-29b [15] and miR-448-3p [16]. MiR-136-5p is one of the miRNAs that has been revealed to be implicated in the progression of glioma [17], while the impact of miR-136-5p on IA remains to be explored. Moreover, it has been reported that NORAD sponged miR-136-5p in non-small cell lung cancer (NSCLC) [18]. However, this regulatory relationship has not been unveiled in IA. Lysine (K)-specific demethylase 1A (KDM1A) is a histone demethylase specifically catalyzing the demethylation of di- and monomethylated lysine 4 in histone 3 by amine oxidation [19]. KDM1A has been unraveled to participate in neuroblastoma [20]. We performed this research to explore the role of NORAD/miR-136-5p/KDM1A axis during IA formation and rupture, and we supposed that NORAD may sponge miR-136-5p to affect the progression of IA with the involvement of KDM1A.

Materials and methods

Ethics statement

Written informed consents were acquired from all patients before this study. The protocol of this study was confirmed by the Ethic Committee of the First Affiliated Hospital of Airforce Medical University and based on the ethical principles for medical research involving human subjects of the Helsinki Declaration.

Study subjects

From June 2014 to January 2019, clinical samples were obtained from IA patients who had undergone surgical resection of IA in the First Affiliated Hospital of Airforce Medical University. Among the 82 samples (35 males, 47 females, 29–80 years old, mean age of 55.27 ± 13.58 years), 49 cases were diagnosed as ruptured IA and the remaining 33 cases as unruptured IA; 55 cases were below 10 mm in tumor diameter and 27 cases were above 10 mm in tumor diameter; 39 cases were anterior circulation aneurysms and 43 cases were posterior circulation aneurysms. All the specimens were confirmed by digital subtraction angiography before operation and tissue sections were confirmed as IA after operation. In addition, normal cerebral artery from 39 patients (16 males and 23 females, aged 33–70 years, mean age of 53.64 ± 10.25 years) with brain trauma were resected. Tissues were frozen to extract total RNA and protein.

Cell culture, grouping, and transfection

Human aortic vascular smooth muscle cells (T/G HA-VSMC, American Type Culture Collection, VA, USA) were cultured in complete Dulbecco's modified Eagle medium (DMEM) containing 10% fetal bovine serum (FBS) in an incubator (Thermo Fisher Scientific Inc., MA, USA). Then, trypsin was used to seed the cells into 6-well plates for 24 h. The cells were, respectively, treated with short hairpin RNA (sh)-NORAD, sh-negative control (NC), overexpressed (oe)-NORAD, oe-NC, miR-136-5p inhibitor, inhibitor NC, oe-NORAD + miR-136-5p mimic, oe-NORAD + mimic NC, oe-NORAD + sh-KDM1A, or oe-NORAD + sh-NC (all from GenePharma Co., Ltd., Shanghai, China) based on instructions of Lipofectamine 2000 reagent (Invitrogen Inc., CA, USA).

Cell counting kit-8 (CCK-8) assay

Cell proliferation was evaluated by CCK-8 assay referring to a publication [21].

Transwell assay

The 24-well plates were placed in 6.5-mm Transwell chambers (aperture diameter of 8 μm). Cells were trypsinized and appended with serum-free DMEM, and then were added into the Transwell apical chambers with 100–300 μL cell suspension/chamber, and about 10^4 cells were counted. After 24-h culture, cells in the apical chambers were discarded and those that migrated were fixed (methanol: glacial acetic acid = 3:1) at 500 μL/well. The cells were stained with a Giemsa

dye solution (mixing ratio at 1:9) for 30–60 min, observed and counted in 5 fields using an inverted microscope.

Scratch test

A maker was used to scratch on the bottom of 12-well plates across the wells. Cell were seeded and when the cell confluence reached 80–90%, a 200 μL yellow pipette tip was used to vertically scratch the cell plate along the ruler. With the medium discarded, cells were continuously cultured, observed, and photographed at 0 and 24 h.

Flow cytometry

VSMCs were resuspended by 100 μL pre-cold 1 × binding buffer and then successively added with 5 μL Annexin and 5 μL propidium iodide (PI) for 15 min. The apoptosis was detected by a flow cytometer (BD Biosciences, NJ, USA).

Reverse transcription quantitative polymerase chain reaction (RT-qPCR)

Total RNA was extracted using Trizol kits (Invitrogen) and cDNA was reversely transcribed by TaqMan MiR cDNA kits (Applied Biosystems Inc., CA, USA). Then, the synthesized cDNA was subjected to PCR using the ABI PRISM 7300 RT-qPCR system and FAST SYBR Green PCR kits (Applied Biosystems) with U6 and glyceraldehyde phosphate dehydrogenase (GAPDA) as the internal references. Data were analyzed using $2^{-\Delta\Delta Ct}$ method and primer sequences were shown in Table 1.

Table 1. Primer sequence.

Genes	Primers (5′-3′)
NORAD	Forward: 5′-TGATAGGATACATCTTGGACATGGA-3′
	Reverse: 5′-AACCTAATGAACAAGTCCTGACATACA-3′
miR-136-5p	Forward: 5′-ACTCCATTTGTTTTGATGATGGA-3′
	Reverse: 5′-CTCTACAGCTATATTGCCAGCCAC-3′
KDM1A	Forward: 5′-AGCATCTGAAGTAAAGCCAC-3′
	Reverse: 5′-AAAGTCATCATCCTGATCCC-3′
U6	Forward: 5′- GCTTCGGCAGCACATATACTAAAA T-3′
	Reverse: 5′-CGCTTCACGAATTTGCGTGTCAT-3′
GAPDH	Forward: 5′-GTCTCCTCTGACTTCAACAGCG-3′
	Reverse: 5′-ACCACCCTGTTGCTGTAGCCAA-3′
SM-MHC	Forward: 5′-AGAGACAGCTTCACGAGTATGAG-3′
	Reverse: 5′-CTTCCAGCTCTCTTTGAAAGTC-3′
SM-α-actin	Forward: 5′- GACCCTGAAGTACCCGATAGAAC-3′
	Reverse: 5′-GGGCAACACGAAGCTCATTG-3′
SM-22α	Forward: 5′-TGAAGGCGGCTGAGGACTAT-3′
	Reverse: 5′-TCTGTTGCTGCCCATCTGAA-3′
MMP-2	Forward: 5′-GCCTGGTCAGTGGCTTGGGGTA-3′
	Reverse: 5′-AGATCTTCTTCTTCAAGGACCGGTT-3′
MMP-3	Forward: 5′-TGTGTGAAAGCAGCAAAGAG-3′
	Reverse: 5′-GCAAGTCTCCTCATTGAATCC-3′
TNF-α	Forward: 5′-AGATGTGGAACTGGCAGAGG-3′
	Reverse: 5′-CCCATTTGGGAACTTCTCCT-3′

Note: NORAD, noncoding RNA activated by DNA damage; miR-136-5p, microRNA-136-5p;KDM1A, lysine-specific demethylase 1A; GAPDH, glyceraldehyde phosphate dehydrogenase; SM-MHC, smooth muscle myosin heavy chain; SM-α actin, smooth muscle α-actin; SM-22α, smooth muscle-22α; MMP-2, matrix metalloproteinase-2; MMP-3, matrix metalloproteinase-3; TNF-α, tumor necrosis factor-α.

Western blot analysis

Proteins in tissues and cells were extracted. The proteins were conducted with 10% sodium dodecyl sulfate-polyacrylamide gel electrophoresis (Boster Biological Technology Co., Ltd., Hubei, China), transferred onto membranes and blocked with 5% bovine serum albumin. The membranes were incubated with the primary antibodies KDM1A (1:500, ab129195, Abcam Inc., MA, USA) and β-actin (1:1000, Santa Cruz Biotechnology Inc, CA, USA) at 4°C overnight. Next, the membranes were incubated with relative secondary antibody (ZSGB-Bio, Beijing, China) for 1 h and developed with enhanced chemiluminescent reagent and the Bio-rad Gel Doc EZ imager (Bio-Rad Laboratories, CA, USA). Gray value of protein bands was analyzed by Image J software with β-actin as the loading control.

Dual luciferase reporter gene assay

Binding site of NORAD and miR-136-5p was predicted by the bioinformatic website Starbase, and that of miR-136-5p and KDM1A was predicted using the RNA22 tool. NORAD 3′-UTR (or KDM1A 3′-UTR) fragment was synthesized and the wild-type (WT) NORAD (or KDM1A) 3′UTR was constructed and named as NORAD-3′UTR-WT (or KDM1A-3′UTR-WT). Then, binding sites were mutated to obtain mutant type (MUT) plasmid: NORAD-3′UTR-MUT (or KDM1A-3′UTR-MUT). Trypsinized VSMCs were transfected with NORAD-3′UTR-WT/NORAD-3′UTR-MUT (or KDM1A-3′UTR-WT/KDM1A-3′UTR-MUT) and miR-136-5p mimic or miR-136-5p mimic NC by

transfection reagent for 48 h. The luciferase activity was detected.

RNA pull-down assay

Three different biotinylated miRNA sequences were designed and synthesized: WT miR-136-5p (miR-136-5p-WT), MUT miR-136-5p (miR-136-5p-MUT, sequence that is complementary to NORAD was mutated) and a random miRNA that is complementary to NORAD (Bio-probe NC). VSMCs were transfected with miR-136-5p-WT, miR-136-5p-MUT and Bio-probe NC for 48 h. Then, cells were lysed to obtain protein lysate, which was incubated with magnetic beads coated with M-280 streptavidin (Sigma) at 4°C for 3 h. The beads were rinsed and the protein-nucleic acid complex was eluted. Trizol was used to extract the RNA and NORAD expression was assessed by RT-qPCR.

Statistical analysis

All data analyses were conducted using the SPSS 21.0 software (IBM Corp. Armonk, NY, USA). The measurement data conforming to the normal distribution were expressed as mean ± standard deviation. The unpaired t-test was performed for comparisons between two groups, one-way analysis of variance (ANOVA) was used for comparisons among multiple groups and Tukey's post hoc test was used for pairwise comparisons after one-way ANOVA. P value <0.05 was indicative of a statistically significant difference.

Results

NORAD and KDM1A are upregulated while miR-136-5p is downregulated in IA, especially in ruptured IA

Phenotypic changes, such as the proliferation of VSMCs, are involved in the pathogenesis of IA [22]. However, the molecular mechanism of VSMC phenotype regulation is still unclear. LncRNA plays a very important role in cell proliferation and apoptosis [23], miRNAs present key functions in many biological processes [24] and KDM1A is a nuclear amine oxidase homologue that regulates transcription [25].

To explore the effects of NORAD, miR-136-5p, and KDM1A on IA, we first compared the expressions of NORAD, miR-136-5p, and KDM1A in IA and normal artery tissues. The IA patients were classified into the ruptured and unruptured IA groups. Patients with unruptured IA had complete wall and generally showed no marked severe symptoms, while those with ruptured IA usually showed sudden and severe symptoms. Our results indicated that (Figure 1a-e) NORAD and KDM1A were upregulated, while miR-136-5p was downregulated in IA patients, especially in ruptured IA patients. NORAD, miR-136-5p, and KDM1A levels were analyzed by Pearson test, and we found that (figure 1f, g) NORAD expression was negatively related to miR-136-5p expression ($r = -0.660$, $P < 0.001$), and miR-136-5p expression was also negatively related to KDM1A expression ($r = -0.663$, $P < 0.001$). These data confirmed that the IA formation and development may be associated with NORAD, miR-136-5p, and KDM1A.

NORAD expression is associated with Hunt–Hess grade, IA diameter, and rupture of IA patients

NORAD in the intracranial aneurysm tissue of IA patients was increased. To further explore the relationship between NORAD and the clinicopathological characteristics of patients with IA, we analyzed the clinical data of IA patients. The IA patients were divided into the high and low-expression groups based on median NORAD expression, and the relationship between NORAD expression and clinicopathological characteristics of IA patients was analyzed. It came out that (Table 2) patients with ruptured IA, IA diameter >10 mm and III-IV Hunt–Hess grade had increased ratio of high NORAD expression. Namely, NORAD expression was related to Hunt–Hess grade, IA diameter, and rupture, while it was not related to age, gender, hypertension history, smoking history, and IA location.

Overexpressed NORAD decelerates apoptosis and accelerates proliferation and migration of VSMCs

To investigate the effect of NORAD on VSMCs, VSMCs were transfected with sh-NORAD or oe-NORAD. We found that sh-NORAD downregulated

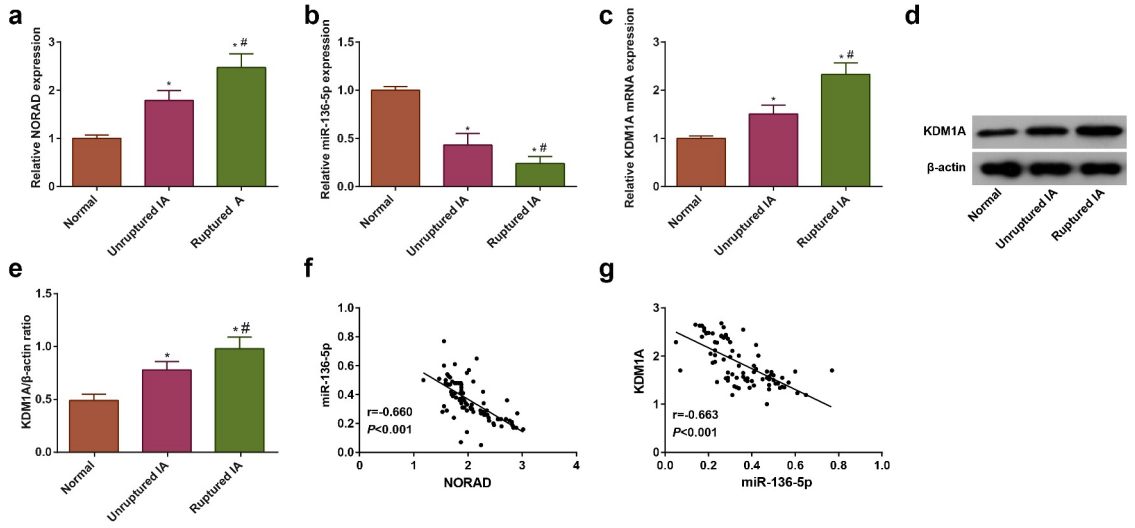

Figure 1. NORAD and KDM1A are upregulated while miR-136-5p is downregulated in IA, especially in ruptured IA. A-C, expression of NORAD, miR-136-5p and KDM1A in unruptured IA (n = 49), ruptured IA (n = 33) and normal artery tissues (n = 39) was determined using RT-qPCR; D-E, KDM1A expression in each tissue was assessed by Western blot analysis; F, Pearson test was used to analyze the relation between NORAD and miR-136-5p in IA; G, Pearson test was used to analyze the relation between KDM1A and miR-136-5p in IA; in Fig. A-E, * $P < 0.05$ *vs* the normal artery tissues, # $P < 0.05$ *vs* unruptured IA; the measurement data conforming to the normal distribution were expressed as mean ± standard deviation, one-way ANOVA was used for comparisons among multiple groups and Tukey's post hoc test was used for pairwise comparisons after one-way ANOVA.

Table 2. Relation between NORAD expression and clinicopathological characteristics of IA patients.

Clinicopathological characteristics	N	NORAD expression		*P*-value
		Low expression (n = 41)	High expression (n = 41)	
Age (year)				
< 50	34	16	18	0.516
≥ 50	48	15	23	
Gender				
Male	35	21	14	0.118
Female	47	20	27	
IA classification				
Unruptured IA	49	30	19	0.013
Ruptured IA	33	11	22	
IA diameter (mm)				
≤ 10	55	32	23	0.034
> 10	27	9	18	
Hypertension history				
Yes	36	17	19	0.628
No	46	24	22	
Smoking history				
Yes	33	15	18	0.499
No	49	26	23	
Blood glucose (mmol/L)				
< 5	59	33	26	0.46
> 5	23	8	15	
Hunt-Hess grade				
I-II	56	34	22	0.004
III-IV	26	7	19	
IA location				
Anterior circular aneurysm	39	22	17	0.269
Posterior circular aneurysm	43	19	24	

Note: NORAD, noncoding RNA activated by DNA damage; IA, intracranial aneurysm. Data in this table are enumeration data and were analyzed by chi-square test.

NORAD, while oe-NORAD upregulated NORAD expression in VSMCs (Figure 2a). Next, we tested the effect of NORAD expression level on the biological activity of VSMCs, and observed that downregulated NORAD suppressed cell proliferation, number of migrated cells and cell wound healing rate, and promoted apoptosis rate; upregulated NORAD had totally reverse effect on VSMCs (Figure 2b-e).

VSMCs present in the media of the aortic wall can be divided into contractile and synthetic types according to their structure and function. The conversion of VSMCs into synthetic cells is

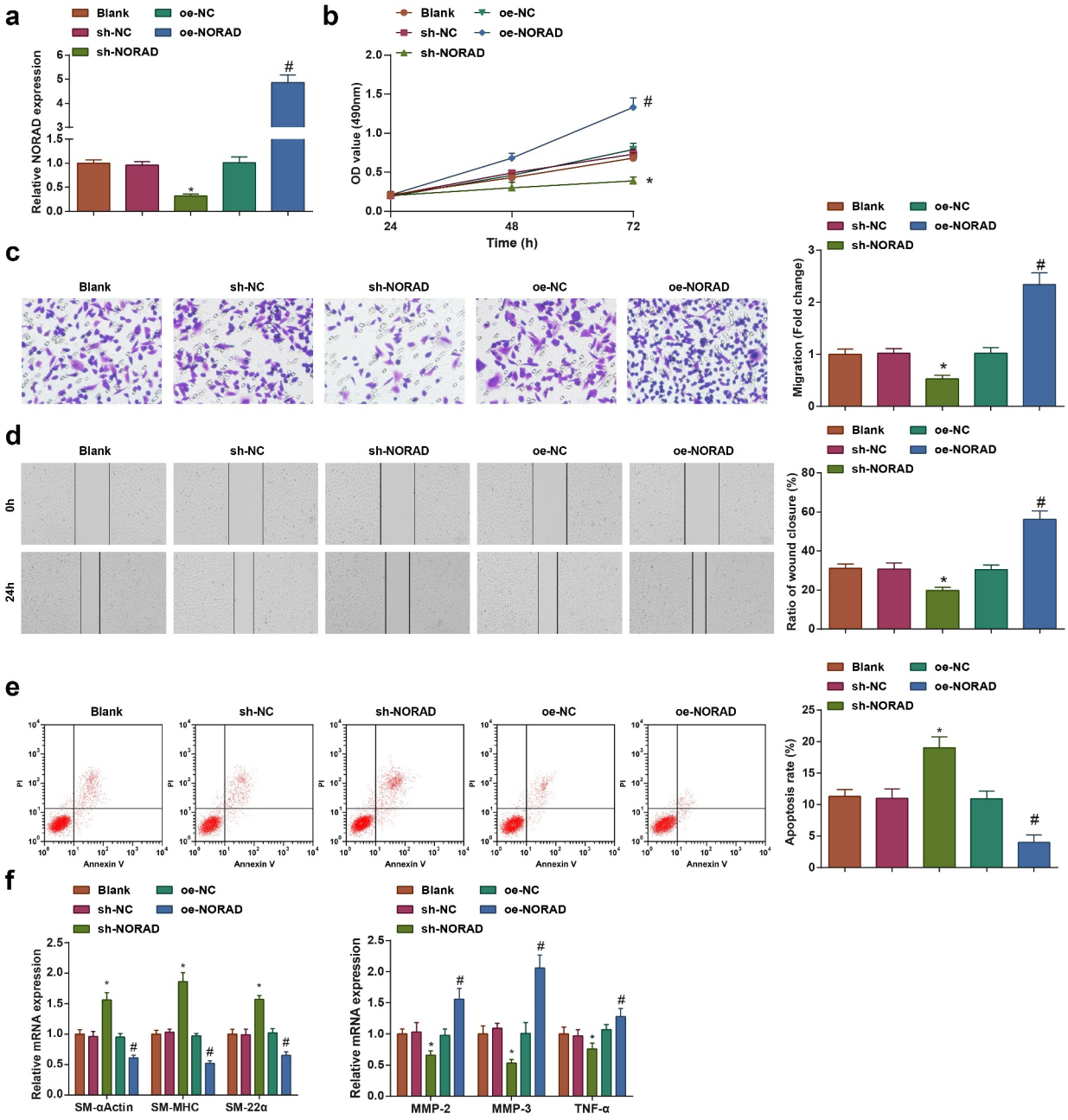

Figure 2. Overexpressed NORAD decelerates apoptosis and accelerates proliferation and migration of VSMCs. A, transfection efficiency of NORAD in VSMCs was evaluated by RT-qPCR; B, viability of VSMCs was assessed by CCK-8 assay; C/D, migration ability of VSMCs was evaluated by Transwell assay and scratch test; E, apoptosis of VSMCs was determined using flow cytometry; F, expression of SM-MHC, SM-α Actin, SM-22α, MMP-2, MMP-3 and TNF-α was measured by RT-qPCR; N = 3; * $P < 0.05$ *vs* the sh-NC group, # $P < 0.05$ *vs* the oe-NC group; the measurement data conforming to the normal distribution were expressed as mean ± standard deviation, one-way ANOVA was used for comparisons among multiple groups and Tukey's post hoc test was used for pairwise comparisons after one-way ANOVA.

a prerequisite for cardiovascular diseases, such as atherosclerosis and restenosis. Therefore, we examined the phenotypic regulation of NORAD on VSMCs though measuring smooth muscle (SM) myosin heavy chain (MHC), SM-α Actin, SM-22α, MMP-2, matrix metalloproteinase (MMP)-2, MMP-3, and tumor necrosis factor (TNF)-α mRNA expression using RT-qPCR. It was demonstrated that down-regulating NORAD elevated SM-MHC, SM-α Actin, and SM-22α, while reduced MMP-2, MMP-3, and TNF-α mRNA expression in VSMCs. On the contrary, up-regulating NORAD had the opposite effects on those indicators (figure 2f). The above results indicated that overexpression of NORAD can enhance the biological activity of VSMCs and inhibit conversion of VSMCs into synthetic cells.

Inhibition of miR-136-5p enhances the biological activity and regulates phenotype of VSMCs

To study the role of miR-136-5p in VSMCs, we used miR-136-5p inhibitor to transfect VSMCs and RT-qPCR tested that miR-136-5p expression was reduced in VSMCs (Figure 3a). Then, it was discovered that in response to inhibited miR-136-5p, VSMCs exhibited promoted proliferation, invasion, migration, and restrained apoptosis, as well as reduced SM-MHC, SM-α Actin, and SM-22α mRNA expression, and raised MMP-2, MMP-3, and TNF-α mRNA expression (Figure 3b-f).

NORAD functions as a competing endogenous RNA (ceRNA) of miR-136-5p and miR-136-5p targets KDM1A

A binding site of miR-136-5p and NORAD was predicted at http://StarBase.sysu.edu.cn/ (Figure 4a), and dual-luciferase reporter gene assay further revealed that (Figure 4b) miR-136-5p mimic remarkably suppressed luciferase activity of NORAD-3′UTR-WT, but cast no obvious effect on luciferase activity of NORAD-3′UTR-MUT. The results of RNA pull-down assay implied that (Figure 4c) NORAD enrichment increased in the miR-163-5p-WT. Outcomes of RT-qPCR indicated that (Figure 4d) sh-NORAD upregulated miR-136-5p but oe-NORAD downregulated miR-136-5p, reflecting that NORAD served as a ceRNA of miR-136-5p in VSMCs.

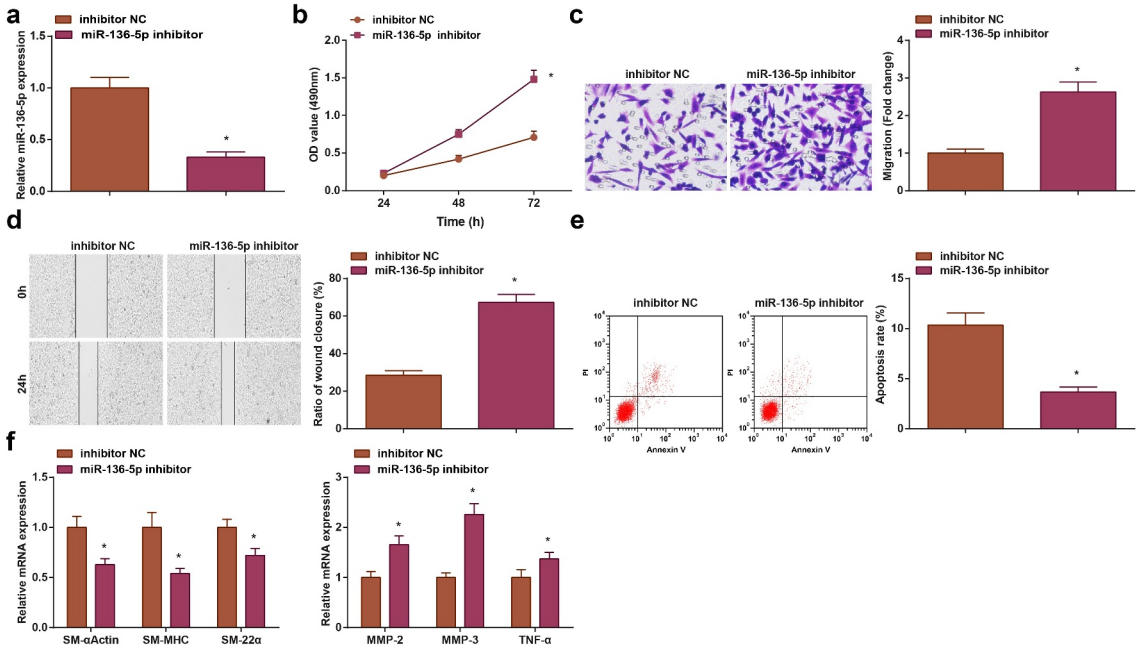

Figure 3. Inhibition of miR-136-5p suppresses VSMC phenotypic switching. A, miR-136-5p expression in VSMCs was detected by RT-qPCR; B, viability of VSMCs was assessed by CCK-8 assay; C/D, migration ability of VSMCs was evaluated by Transwell assay and scratch test; E, apoptosis of VSMCs was determined using flow cytometry; F, expression of SM-MHC, SM-α Actin, SM-22α, MMP-2, MMP-3 and TNF-α was measured by RT-qPCR; N = 3; * $P < 0.05$ *vs* the inhibitor NC group; the measurement data conforming to the normal distribution were expressed as mean ± standard deviation, unpaired t test was used for data comparisons.

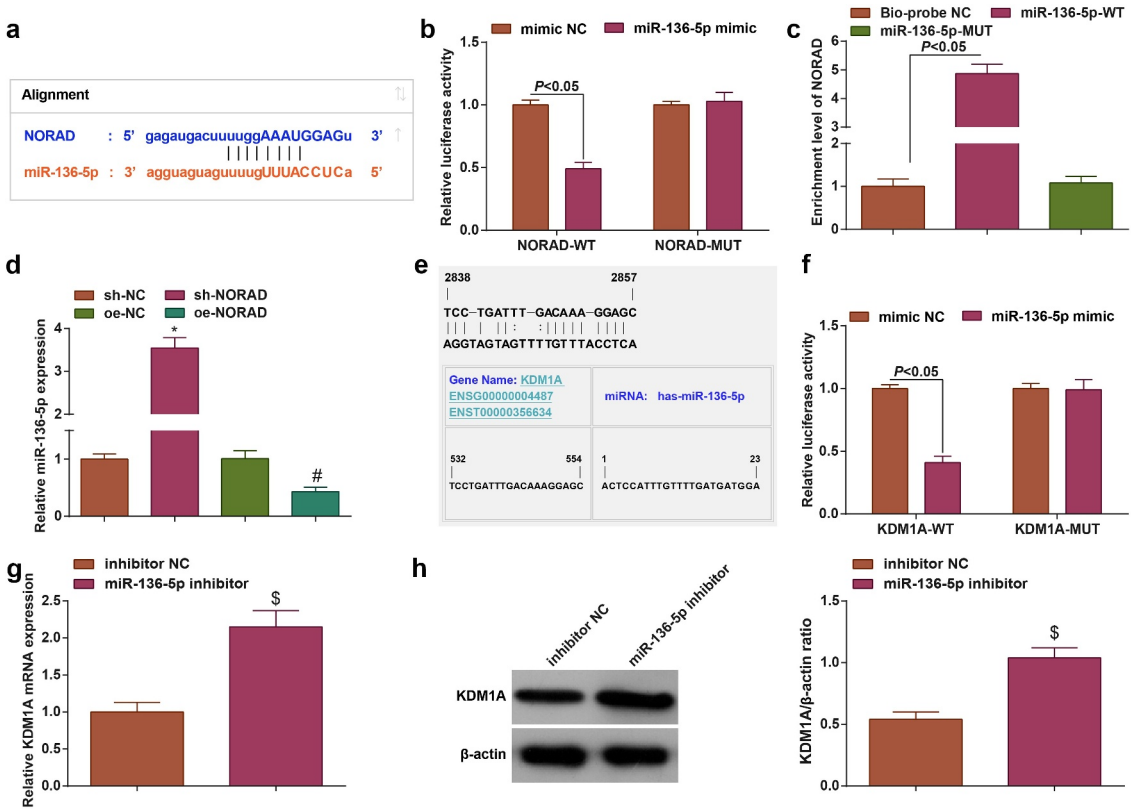

Figure 4. NORAD functions as a ceRNA of miR-136-5p and miR-136-5p targets KDM1A. A, binding site of NORAD and miR-136-5p; B, regulatory relation between NORAD and miR-136-5p was confirmed by dual luciferase reporter gene assay; C, binding relation between NORAD and miR-136-5p was assessed by RNA pull-down assay; D, miR-136-5p expression in VSMCs was determined by RT-qPCR; E, binding site of KDM1A and miR-136-5p; F, regulatory relation between KDM1A and miR-136-5p was confirmed by dual luciferase reporter gene assay; G, KDM1A expression in VSMCs was determined by RT-qPCR; H, protein expression of KDM1A in VSMCs was determined by Western blot analysis; N = 3; & $P < 0.05$ *vs* the inhibitor NC group, the measurement data conforming to the normal distribution were expressed as mean ± standard deviation, unpaired t-test was performed for comparisons between two groups, one-way ANOVA was used for comparisons among multiple groups and Tukey's post hoc test was used for pairwise comparisons after one-way ANOVA.

Meanwhile, the binding site of miR-136-5p and KDM1A was predicted at https://cm.jefferson.edu/rna22/Precomputed/ (Figure 4e). It was confirmed by dual-luciferase reporter gene assay that (figure 4f) there existed a targeting relationship between miR-136-5p and KDM1A. The expression of KDM1A was assessed and we found that (Figure 4g, h) miR-136-5p inhibitor transfection in VSMCs suppressed the KDM1A expression, suggesting a targeting relationship between miR-136-5p and KDM1A.

Upregulated miR-136-5p or reduced KDM1A reverses effect of NORAD overexpression on VSMC phenotypes

Next, the effect of NORAD/miR-136-5p/KDM1A on the development of IA was further explored. We transfected VSMCs with oe-NORAD + miR-136-5p mimic or oe-NORAD + sh-KDM1A. It was observed through RT-qPCR and Western blot that on the basis of oe-NORAD, further transfection of miR-136-5p mimic upregulated miR-136-5p and downregulated KDM1A in

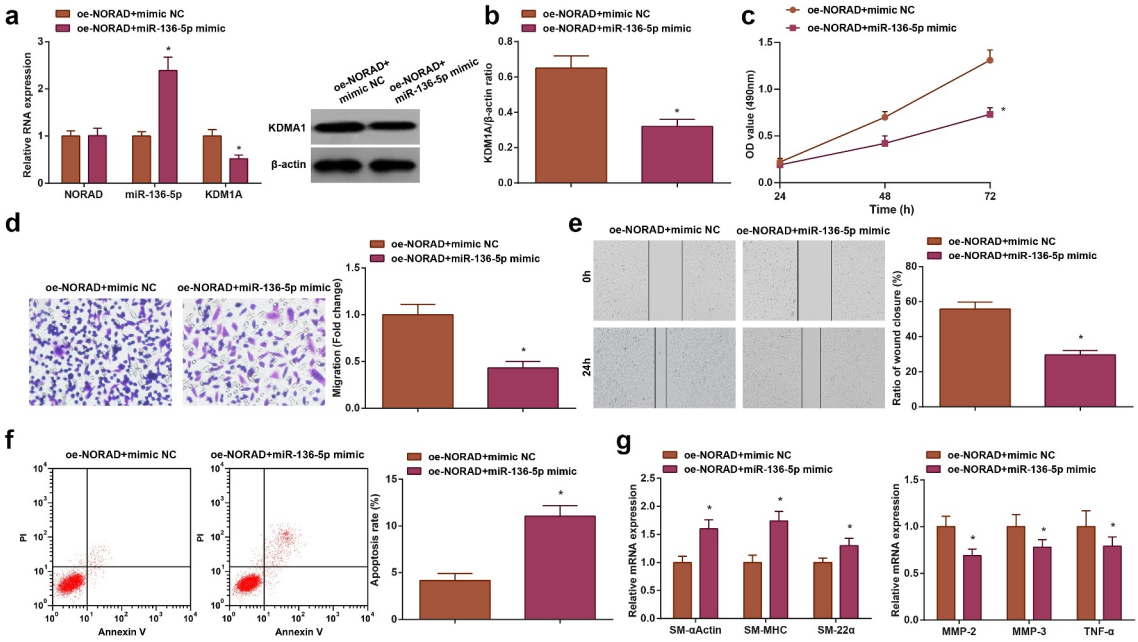

Figure 5. Upregulated miR-136-5p reverses effect of NORAD overexpression on VSMC phenotypes. A, RT-qPCR was used to determine expression of NORAD, miR-136-5p and KDM1A in VSMCs; B, protein expression of KDM1A in VSMCs was detected by Western blot analysis; C, viability of VSMCs was assessed by CCK-8 assay; D/E, migration ability of VSMCs was evaluated by Transwell assay and scratch test; F, apoptosis of VSMCs was determined using flow cytometry; G, expression of SM-MHC, SM-α Actin, SM-22α, MMP-2, MMP-3 and TNF-α was measured by RT-qPCR; N = 3; * $P < 0.05$ *vs* the oe-NORAD + mimic NC group; the measurement data conforming to the normal distribution were expressed as mean ± standard deviation, unpaired t test was used for data comparisons.

VSMCs (Figure 5a, b); while further transfection of sh-KDM1A reduced KDM1A expression (Figure 6a, b). Moreover, miR-136-5p mimic or sh-KDM1A transfection reversed oe-NORAD-mediated promotion of the biological activity of VSMCs (Figure 5c-F; Figure 6c-f). On the other hand, miR-136-5p mimic or sh-KDM1A transfection reversed oe-NORAD-mediated effect on contraction and synthesis-specific indicators, causing SM-MHC, SM-α Actin, and SM-22α mRNA expression to elevate and MMP-2, MMP-3, and TNF-α mRNA to reduce (Figure 5g; Figure 6g). The above data reflected that up-regulating miR-136-5p or suppressing KDM1A reversed the effect of NORAD overexpression on VSMC phenotypes.

Discussion

IA is as an outpouching of a weakened portion of the intracranial vessel wall. Most of IAs are symptom-free, whereas the IA rupture is able to result in fatal consequences [26]. We aim to explore the role of NORAD sponging miR-136-5p in the formation and rupture of IA by regulating KDM1A, and our results revealed that NORAD suppressed miR-136-5p, thus upregulating KDM1A to participate in IA formation and rupture by promoting proliferation and migration, and inhibiting apoptosis of VSMCs.

We assessed NORAD expression in IA and normal cerebral artery tissues, and it came out that NORAD was upregulated in IA, especially in ruptured IA. Similarly, Zhang *et al.* have found that NORAD expression was markedly increased in CRC tissues [12], and it has been revealed that NORAD was upregulated in breast cancer tissues and cells, respectively, versus non-tumor tissues and normal mammary cell line [13]. We down-regulated or up-regulated NORAD to observe their altered roles in the biological functions of VSMCs. Results of the gain- and loss-of-function assay suggested that NORAD silencing promoted proliferation and migration, induced apoptosis, elevated SM-MHC, SM-α Actin, and SM-22α mRNA but reduced MMP-2, MMP-3, and TNF-α mRNA expression in VSMCs. On the other hand, NORAD overexpression functioned oppositely. In line with this finding, Zhang *et al.* have found that

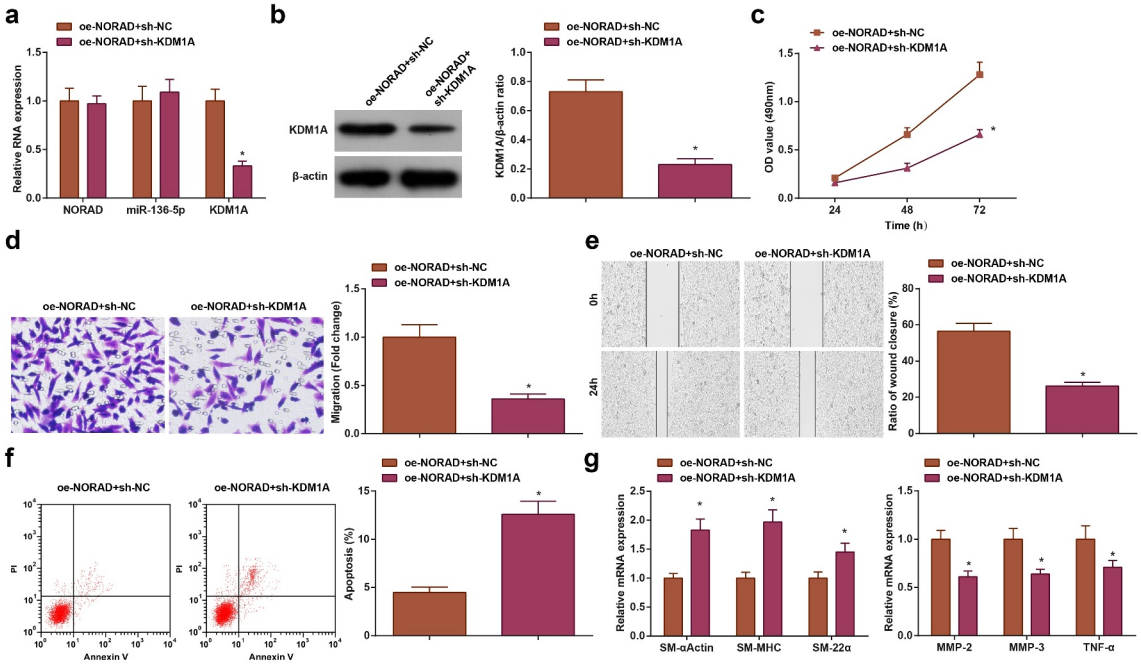

Figure 6. Reduced KDM1A reverses effect of NORAD overexpression on VSMC phenotypes. A, RT-qPCR was used to determine expression of NORAD, miR-136-5p and KDM1A in VSMCs; B, protein expression of KDM1A in VSMCs was detected by Western blot analysis; C, proliferation of VSMCs was assessed by CCK-8 assay; D/E, migration ability of VSMCs was evaluated by Transwell assay and scratch test; F, apoptosis of VSMCs was determined using flow cytometry; G, expression of SM-MHC, SM-α Actin, SM-22α, MMP-2, MMP-3 and TNF-α was measured by RT-qPCR; N = 3; * $P < 0.05$ *vs* the oe-NORAD + sh-NC group; the measurement data conforming to the normal distribution were expressed as mean ± standard deviation, unpaired t test was used for data comparisons.

NORAD-induced proliferation and migration of prostate cancer cells [27], and a recent literature has revealed that NORAD inhibition suppressed proliferation and migration of ovarian cancer cells [28]. Consistently, it has been figured out that the suppression of NORAD facilitated the apoptosis of cancer cells [29], but overexpression of NORAD inhibited apoptosis of gastric cancer cells [30].

LncRNAs can serve as sponges of miRNAs by interacting through common response elements, leading to the regulation of the miRNA activity [31]. Gao *et al.* have elucidated that NORAD promoted cell proliferation and glycolysis in NSCLC by serving as a sponge of miR-136-5p [18], and it has been recently confirmed that NORAD promoted the development of retinoblastoma by sponging miR-136-5p [32]. Consistently, we detected that NORAD functioned as a ceRNA of miR-136-5p and negatively regulated miR-136-5p expression. In our study, miR-136-5p was down-regulated in IA patients, and inhibition of miR-136-5p resulted in enhanced biological functions of VSMCs and induced imbalance between contraction and synthesis-specific factors. In fact, miR-136-5p has been revealed to be downregulated in glioma [17]. Accordingly, it has also been validated that miR-136-5p repressed cell proliferation and migration in renal cell carcinoma [33]. Moreover, a publication has reported that miR-136 contributed to the apoptosis of gastric cancer cells [34], and miR-136 was able to accelerate the apoptosis of glioma cells [35].

miRNAs are known to regulate target gene expression via binding the 3′UTR of target mRNA [36]. Outcomes of our research indicated that KDM1A was a target gene of miR-136-5p, and KDM1A was up-regulated in IA. Functionally, we discovered that silencing KDM1A reversed the effect of restored NORAD on VSMCs. Indeed, Althoff *et al.* have validated that KDM1A was highly expressed in neuroblastomas [20]. In addition, KDM1A expression is high in triple negative breast cancer and suppression of KDM1A reduced cell viability and promoted apoptosis of cancer stem cells [37]. Moreover, elevated KDM1A was measured in papillary thyroid cancer and suppressing the level of KDM1A limited migration and invasion of tumor cells [38]. Actually,

Xiaobo Zhang *et al.* have discussed that KDM1A knockdown prevents VSMCs from transforming into synthetic phenotype and reduces proliferation of VSMCs [39].

Taken together, our research unveiled that NORAD reduction upregulated miR-136-5p to suppress the progression of IA by inhibiting KDM1A, and the elevation of miR-136-5p or silenced KDM1A was able to reverse the effect of overexpressed NORAD on VSMCs. This study may contribute to the understanding of IA mechanisms and renewed the possible reference for clinical treatment for IA. However, more efforts are needed for further study to confirm and develop our study results.

Acknowledgement

We would like to acknowledge the reviewers for their helpful comments on this paper.

Disclosure statement

No potential conflict of interest was reported by the author(s).

Funding

This work was supported by the Xijing Hospital Discipline Promotion Program [XJZT19MJ39].

Conflict of interest

The authors declare that they have no conflicts of interest.

References

[1] HaiFeng L, YongSheng X, YangQin X, et al. Diagnostic value of 3D time-of-flight magnetic resonance angiography for detecting intracranial aneurysm: a meta-analysis. Neuroradiology. 2017;59(11):1083–1092.

[2] Thomas B, Guo D. The Diagnostic Accuracy of Evoked Potential Monitoring Techniques During Intracranial Aneurysm Surgery for Predicting Postoperative Ischemic Damage: a Systematic Review and Meta-Analysis. World Neurosurg. 2017;103:829–840. [e3].

[3] Jin D, Song C, Xiaolei L, et al. A systematic review and meta-analysis of risk factors for unruptured intracranial aneurysm growth. Int J Surg. 2019;69:68–76.

[4] Chen X, Yun L, Huazhang T, et al. Meta-analysis of computed tomography angiography versus magnetic resonance angiography for intracranial aneurysm. Medicine (Baltimore). 2018;97(20):e10771.

[5] Tromp G, Weinsheimer S, Ronkainen A, et al. Molecular basis and genetic predisposition to intracranial aneurysm. Ann Med. 2014;46(8):597–606.

[6] Lai LT, O'Neill AH. History, Evolution, and Continuing Innovations of Intracranial Aneurysm Surgery. World Neurosurg. 2017;102:673–681.

[7] Backes D, Rinkel G, Laban KG, et al. Patient- and Aneurysm-Specific Risk Factors for Intracranial Aneurysm Growth: a Systematic Review and Meta-Analysis. Stroke. 2016;47(4):951–957.

[8] Marbacher S, Niemelä Mika, Hernesniemi Juha, et al. Recurrence of endovascularly and microsurgically treated intracranial aneurysms-review of the putative role of aneurysm wall biology. Neurosurg Rev. 2019;42(1):49–58.

[9] Sun M, Nie Fengqi, Wang Yunfei, et al. LncRNA HOXA11-AS Promotes Proliferation and Invasion of Gastric Cancer by Scaffolding the Chromatin Modification Factors PRC2, LSD1, and DNMT1. Cancer Res. 2016;76(21):6299–6310.

[10] Wu C, Song Hailong, Wang Yinzhou, et al. Long non-coding RNA TCONS_00000200 as a non-invasive biomarker in patients with intracranial aneurysm. Biosci Rep. 2019;**39**(11):1-11.

[11] Man H, Bi W. Expression of a Novel Long Noncoding RNA (lncRNA), GASL1, is Downregulated in Patients with Intracranial Aneurysms and Regulates the Proliferation of Vascular Smooth Muscle Cells In Vitro. Med Sci Monit. 2019;25:1133–1139.

[12] Zhang J, Li Xiao-Yan, Hu Ping, et al. LncRNA NORAD contributes to colorectal cancer progression by inhibition of miR-202-5p. Oncol Res. 2018;26(9):1411–1418.

[13] Zhou K, Ou Qin, Wang Geng, et al. High long non-coding RNA NORAD expression predicts poor prognosis and promotes breast cancer progression by regulating TGF-beta pathway. Cancer Cell Int. 2019;19(1):63.

[14] Wang Y, Yuan Yitong, Gao Yuantao, et al. MicroRNA-31 regulating apoptosis by mediating the phosphatidylinositol-3 kinase/protein kinase B signaling pathway in treatment of spinal cord injury. Brain Dev. 2019;41(8):649–661.

[15] Sun L, Zhao Manman, Zhang Jingbo, et al. MiR-29b Downregulation Induces Phenotypic Modulation of Vascular Smooth Muscle Cells: implication for Intracranial Aneurysm Formation and Progression to Rupture. Cell Physiol Biochem. 2017;41(2):510–518.

[16] Zhang JZ, Chen Dan, Lv Li-Quan, et al. miR-448-3p controls intracranial aneurysm by regulating KLF5 expression. Biochem Biophys Res Commun. 2018;505(4):1211–1215.

[17] Li DX, Fei XR, Dong YF, et al. The long non-coding RNA CRNDE acts as a ceRNA and promotes glioma malignancy by preventing miR-136-5p-mediated downregulation of Bcl-2 and Wnt2. Oncotarget. 2017;8(50):88163–88178.

[18] Gao W, Weng Ting, Wang Lifan, et al. Long noncoding RNA NORAD promotes cell proliferation and glycolysis in nonsmall cell lung cancer by acting as a sponge for miR1365p. Mol Med Rep. 2019;19 (6):5397–5405.
[19] Shi Y, Lan Fei, Matson Caitlin, et al. Histone demethylation mediated by the nuclear amine oxidase homolog LSD1. Cell. 2004;119(7):941–953.
[20] Althoff K, Beckers Anneleen, Odersky Andrea, et al. MiR-137 functions as a tumor suppressor in neuroblastoma by downregulating KDM1A. Int J Cancer. 2013;133(5):1064–1073.
[21] Luo J, Jin Hengwei, Jiang Yuhua, et al. Aberrant Expression of microRNA-9 Contributes to Development of Intracranial Aneurysm by Suppressing Proliferation and Reducing Contractility of Smooth Muscle Cells. Med Sci Monit. 2016;22:4247–4253.
[22] Yin K, Liu X. Circ_0020397 regulates the viability of vascular smooth muscle cells by up-regulating GREM1 expression via miR-502-5p in intracranial aneurysm. Life Sci. 2021;265:118800.
[23] Fu D, Yang S, Lu J, et al. LncRNA NORAD promotes bone marrow stem cell differentiation and proliferation by targeting miR-26a-5p in steroid-induced osteonecrosis of the femoral head. Stem Cell Res Ther. 2021;12 (1):18.
[24] Yang X, Peng Jianhua, Pang Jinwei, et al. A functional polymorphism in the promoter region of miR-155 predicts the risk of intracranial hemorrhage caused by rupture intracranial aneurysm. J Cell Biochem. 2019;120(11):18618–18628.
[25] Maes T, Mascaró Cristina, Tirapu Iñigo, et al. ORY-1001, a Potent and Selective Covalent KDM1A Inhibitor, for the Treatment of Acute Leukemia. Cancer Cell. 2018;33(3):495–511. e12.
[26] Shin YW,Yong-Won, Park, et al. Association of Bone Mineral Density With the Risk of Intracranial Aneurysm. JAMA Neurol. 2018;75(2):179–186.
[27] Zhang H, Guo H. Long non-coding RNA NORAD induces cell proliferation and migration in prostate cancer. J Int Med Res. 2019;47(8):3898–3904.
[28] Xu C, Zhu LX, Sun DM, et al. Regulatory mechanism of lncRNA NORAD on proliferation and invasion of ovarian cancer cells through miR-199a-3p. Eur Rev Med Pharmacol Sci. 2020;24(4):1672–1681.
[29] Li J, Xu Xia, Wei Cungang, et al. Long noncoding RNA NORAD regulates lung cancer cell proliferation, apoptosis, migration, and invasion by the miR-30a-5p/ADAM19 axis. Int J Clin Exp Pathol. 2020;13(1):1–13.
[30] Tao W, Li Yajun, Zhu Meng, et al. LncRNA NORAD Promotes Proliferation And Inhibits Apoptosis Of Gastric Cancer By Regulating miR-214/Akt/mTOR Axis. Onco Targets Ther. 2019;12:8841–8851.
[31] Tang Y, Cheng-xing, Xiang, et al. The lncRNA MALAT1 protects the endothelium against ox-LDL-induced dysfunction via upregulating the expression of the miR-22-3p target genes CXCR2 and AKT. FEBS Lett. 2015;589(20 Pt B):3189–3196.
[32] Yang XL, Hao Y-J, Wang B, et al. Long noncoding RNA NORAD promotes the progression of retinoblastoma by sponging miR-136-5p/PBX3 axis. Eur Rev Med Pharmacol Sci. 2020;24(3):1278–1287.
[33] Chen P, Zhao Liwen, Pan Xiang, et al. Tumor suppressor microRNA-136-5p regulates the cellular function of renal cell carcinoma. Oncol Lett. 2018;15 (4):5995–6002.
[34] Yu L, Zhou GQ, Li DC. MiR-136 triggers apoptosis in human gastric cancer cells by targeting AEG-1 and BCL2. Eur Rev Med Pharmacol Sci. 2018;22 (21):7251–7256.
[35] Yang Y, Wu Jueheng, Guan Hongyu, et al. MiR-136 promotes apoptosis of glioma cells by targeting AEG-1 and Bcl-2. FEBS Lett. 2012;586(20):3608–3612.
[36] Fang YY, Tan Ming-Rong, Zhou Jian, et al. miR-214-3p inhibits epithelial-to-mesenchymal transition and metastasis of endometrial cancer cells by targeting TWIST1. Onco Targets Ther. 2019;12:9449–9458.
[37] Zhou M, Venkata Prabhakar Pitta, Viswanadhapalli Suryavathi, et al. KDM1A inhibition is effective in reducing stemness and treating triple negative breast cancer. Breast Cancer Res Treat. 2021;185(2):343–357.
[38] Zhang W, Sun Wei, Qin Yuan, et al. Knockdown of KDM1A suppresses tumour migration and invasion by epigenetically regulating the TIMP1/MMP9 pathway in papillary thyroid cancer. J Cell Mol Med. 2019;23 (8):4933–4944.
[39] Zhang X, Huang Tao, Zhai Heng, et al. Inhibition of lysine-specific demethylase 1A suppresses neointimal hyperplasia by targeting bone morphogenetic protein 2 and mediating vascular smooth muscle cell phenotype. Cell Prolif. 2020;53(1):e12711.